FlexRICAN
Flexibility in RIs for global CArbon Neutrality

This project has received funding from the European Union's Horizon Europe research and innovation programme's HORIZON-INFRA-2023-TECH-01 call under Grant Agreement No. 101131516

Deliverable

D3.1 Solar Panel pre-cooling

Project Deliverable Information Sheet

FlexRICAN Project	Project Ref. No. **101131516**	
	Project Title: **FlexRICAN – Flexibility in RIs for global CArbon Neutrality**	
	Project Website: **https://flexrican.eu/**	
	Work Package: **WP3**	
	Deliverable: **D3.1 Solar Panel pre-cooling**	
	Deliverable Type: **Report**	
	Dissemination Level: **Public**	Contractual Delivery Date: **31.08.2025**
		Actual Delivery Date: **27.08.2025**
	EC Project Officer: **Andreas Holtel**	

Document Control Sheet

Document	Title: **Solar Panel pre-cooling**	
	Version: **1.0**	
	Available at: **https://flexrican.eu/**	
	Files: **1**	
Authorship	Written by	**Diego Herrera Ruiz (ESS)**
	Contributors	**Gergely Samu (ELI ALPS), Marion Perrin (EP), Peyman Olad (ESS)**
	Reviewed by	**FlexRICAN Steering Board**
	Approved	**FlexRICAN General Assembly**

Table of Contents

List of Abbreviations and Acronyms

AL	Alfa Laval
CB	Conduction Band
CNRS	Centre National De La Recherche Scientifique
ELI	Extreme Light Infrastructure ERIC
EMFL	European Magnetic Field Laboratory
EP	Energy Pool
ERIC	European Research Infrastructure Consortium
ESRFI	European Strategy Forum on Research Infrastructures
ESS	European Spallation Source ERIC
EVA	Ethylene Vinyl Acetate
FF	Fill Factor
FlexRICAN	Flexibility in Research Infrastructures for Global Carbon Neutrality
HZDR	Helmholtz-Zentrum Dresden-Rossendorf
Jsc	Short Circuit Current
PCE	Power Conversion Efficiency
PCM	Phase Change Material
PV	Photovoltaic
RI	Research Infrastructure
ROI	Return of investment
Si	Silicon
SRU	Stichting Radboud Universiteit
VB	Valence Band
Voc	Open Circuit Voltage

Executive Summary

The **FlexRICAN** project (Flexibility in Research Infrastructures for Global Carbon Neutrality) aims to transform energy use across large-scale European research infrastructures (RIs) by enhancing energy flexibility, efficiency, and sustainability. Coordinated across eight European partners, including three major ESFRI infrastructures: **ESS (Sweden), ELI (Czech Republic/Hungary), and EMFL (France/Germany/Netherlands);** the project seeks to reduce the carbon footprint of these high-energy-demand facilities through integrated, multi-energy solutions.

A key component of the project is **Work Package 3**, which investigates the potential for on-site renewable energy generation, particularly **solar photovoltaics (PV)**, and explores the performance gains achievable through **active cooling of PV panels**. Using ESS as a test site, the study explores the use of **backside water cooling systems** to mitigate the temperature-induced performance losses common in PV panels.

Results show that maintaining panel temperatures at 25°C—especially during peak summer months—can lead to **6% increase in annual energy yield**. For a 3.5 MW installation, this equates to **an additional 240 MWh annually**, roughly the consumption of **100 apartments in Sweden**.

A comparative review of conventional PV, hybrid PV-thermal, and cooling-enhanced PV systems indicates that **cooling-focused solutions offer superior electrical performance**. Prototypes will now be built and tested at scale to validate these findings and help define future energy strategies for RIs across Europe.

Introduction

About FlexRICAN

The Project

The Flexibility in Research Infrastructures for Global Carbon Neutrality (FlexRICAN) project aims to transform energy usage within European research infrastructures by bringing together three prominent members of the European Strategy Forum on Research Infrastructures (ESFRI), each with distinct current and future energy demands: the European Spallation Source ERIC (ESS) in Lund, Sweden; the Extreme Light Infrastructure ERIC (ELI), with operational facilities in Prague, Czechia, and Szeged, Hungary; and the European Magnetic Field Laboratory AISBL (EMFL), which includes three DC field facilities—Laboratoire National des Champs Magnétiques Intenses (LNCMI) in Grenoble, France; the Dresden High Magnetic Field Laboratory (HLD) in Dresden, Germany; and the High Field Magnet Laboratory (HFML) in Nijmegen, Netherlands.

Key beneficiaries include the Centre National de la Recherche Scientifique (CNRS) in Toulouse, France; Helmholtz-Zentrum Dresden-Rossendorf (HZDR) in Dresden, Germany; and Stichting Radboud Universiteit (SRU) in Nijmegen, Netherlands. Additionally, two industrial partners—Alfa Laval (AL) and Energy Pool (EP)—bring essential expertise from the energy sector. Through collaborative efforts, the consortium aims to optimize energy management, enhance resource efficiency, and reduce environmental impacts across these infrastructures. Together, the research infrastructures and partners involved in FlexRICAN leverage their collective strengths to support both ongoing and future energy transition initiatives.

Objective

FlexRICAN will demonstrate how research infrastructures, as electricity-intensive actors, can enhance energy flexibility for the European electrical grid and contribute to local heating networks through waste heat recovery projects.

Developing renewable energy production capacity and managing these developments in an integrated way, through energy-oriented modelling that involves RI user communities and new stakeholders, appears to be a promising solution.

Through the development of a multi-energy approach that integrates academic knowledge with the expertise of two key energy-sector actors, FlexRICAN will propose new technologies and solutions to increase resource efficiency and reduce the environmental impacts of European Research Infrastructures (RIs). The project will focus on assessing and validating the implementation of new solutions and technologies at the three ESFRI infrastructures involved.

Prototypes and solutions could be developed and tested at the actual scale of these infrastructures, contributing to the quantification of energy services and the reduction of carbon footprints throughout their full life cycle. These efforts aim to enhance the long-term sustainability of European RIs and strengthen the resilience of the European energy system [1,2].

Project Summary

With a timeline of 36 months and 8 partners from Europe, FlexRICAN is divided into nine different work packages (see **Figure 1**) and will provide:

- New technologies and solutions to increase resource use efficiency and reduce the environmental impacts of European Research Infrastructures.
- Tested prototypes and solutions to identify solutions at an infrastructural scale.
- Assessment and validation for implementation of new solutions and technologies at the three ESFRI infrastructures involved: ESS, ELI and EMFL.
- Increase the long-term sustainability of European Research Infrastructures and contribute to the resilience of the energy systems in Europe.

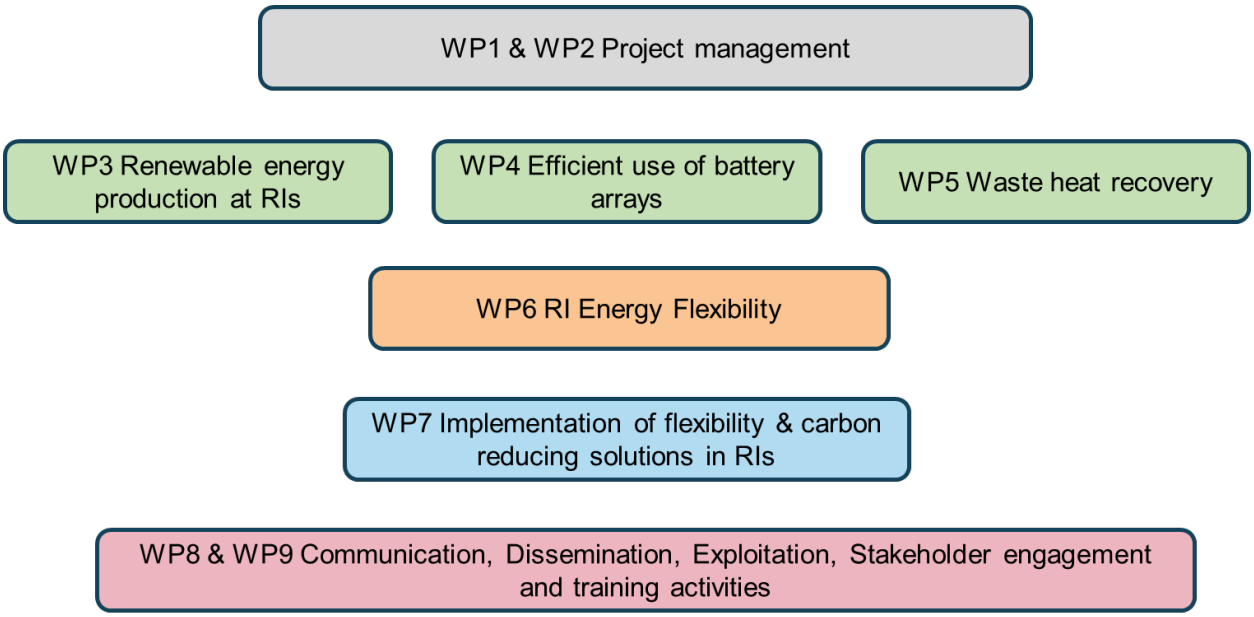

Figure 1: The FlexRICAN project is divided into nine Work Packages (WP) [3].

Work Package 3

Definition of Work Package (WP)

Solar, biogas, and wind power generation can help power RI's. Since RIs occupy substantial real estate, significant power can be generated by using the available space at RIs. The WP will study how solar power can be implemented and how much power can be generated in different configurations. This can then be applied to an RI when the geometry and the meteorological data are known. Cooling the solar panels can improve the performance of a solar power installation, and this will be studied in a sub-task. In another sub-task, alternative energy sources, like wind turbines, will be considered to back up the local grid. The use of solar power can be combined with the use of batteries (WP 4) to increase flexibility and together provide a more reliable grid environment.

Definition of Task

ESS will investigate the use of cooling water to reduce the panel temperature by installing a back cooling system on the panels.

Panel performance efficiency decreases when the surface temperature rises and on a sunny day, significant amount of energy can easily be lost when the panels are heated to more than 50°C. ESS will retrofit a panel together with a producer, build a simple prototype of the panel, and test it to measure the electricity production at different panel temperatures.

The work will include designing how cooling channels run either through or under the panel surface, what flows will work without damaging the pipes, and how electrical safety is ensured [3].

Background and Motivation

An overview of how PV devices work and the relevant parameters that should be monitored for future testing of a prototype are explained in this section.

Photovoltaic Technology

In general terms, the solar photovoltaic energy generation process in semiconductor materials consists of four main steps: Illumination of the material, free charge carrier generation, charge transfer, and charge collection. The process begins when an incident photon with sufficient energy reaches the active layer and excites an electron to a higher energy level. The electron leaves a hole (positive charge) behind when it is excited to a higher energy level, and this hole is paired to the electron by a coulombic force, which creates an exciton or an electron-hole pair. Then, to generate electricity, the free charge carriers need to be collected before they recombine, and the system returns to its ground state (original energy level).

Charge carrier separation and extraction happen at the p-n junction. This is where two types of semiconductor materials, a donor and an acceptor, are combined. The donor has electrons close to its valence band (VB) that can be removed from their bound state and sent into a free state at the lowest empty conduction band (CB) in the acceptor. The energy difference between these energy levels defines the energy required to extract an electron from the CB level so that it can reach the VB level. The value of the energy gap between the two bands, or bandgap, usually ranges from 0.5 eV to 3.0 eV, depending on the materials being used [4-13].

Band Gap

The bandgap energy can be described by **Eq. 1.**

$$E_g = E_g(0) - \frac{\alpha T^2}{\beta + T} \qquad \text{Eq. 1}$$

Where Eg(0) is the bandgap at absolute zero (1.17 eV for Silicon), and α and β are constants for the material (4.73 x 10^{-4} eV/K and 636 K for Silicon) [5].

For wider bandgaps, higher energy is required to excite an electron from the VB, but once separated, it will be more difficult for it to recombine, so radiative losses and photon re-emission decrease. For smaller bandgaps, it is easier to excite electrons from the VB since less energy is required, but there will be more recombination. This translates into less exciton generation for high bandgaps and higher radiative losses for narrow bandgaps [6,7].

This trade-off implies that there isn't a need to increase or decrease the bandgap to improve the performance of a solar cell but rather find that ideal level for which the material performs at its best [4, 6-8].

Short Circuit Current (J_{SC})

The short circuit current (J_{SC}) is the photocurrent generated by the PV device when it is under illumination and at short circuit conditions. This means that there is no external voltage applied to the device, i.e. V = 0. The fact that there is no external bias means that the current is generated solely by the incident light (disregarding the dark current, so $J_{Dark} = 0$. See Eq. 3); thus, defining the maximum value for the current that can be extracted from the PV device. This is also known as the photocurrent of the device [8].

$$J_{Dark} = J_0 \left[\exp\left(\frac{qV}{kT}\right) - 1\right] \quad \text{Eq. 2}$$

$$J(V) = J_{SC} - J_{Dark} \quad \text{Eq. 3}$$

The photocurrent density can also be defined using the external quantum efficiency (QE), which correlates the number of incident photons, without removing reflection losses, and the number of excitons generated by these photons (Eq. 4).

$$J_{SC} = q \int \alpha(\hbar\omega)\mathrm{d}j_\gamma = q \int b_s(E)\, QE(E) dE \quad \text{Eq. 4}$$

where q is the electron's charge, α is the absorptance coefficient over the diffusion length (dependent on the photon's energy $\hbar\omega$), dj_γ is the photocurrent density, and b_s is the incident spectral photon flux density [9].

Open Circuit Voltage (V_{OC})

The open circuit voltage (V_{OC}) represents the voltage available when the terminals of the PV device are isolated, which means that the total current that is going through the device is zero. This parameter defines the maximum value for the voltage that can be generated by the device and its analytical expression (Eq. 5) can be derived easily by substituting J(V)=0 in Eq. 3.

$$V_{OC} = \frac{kT}{q} ln \left(\frac{J_{SC}}{J_0} + 1\right) \quad \text{Eq. 5}$$

The open circuit voltage can also be defined as the energy difference between the electron and hole levels minus the voltage loss caused by the recombination of excitons (see **Figure 2**).

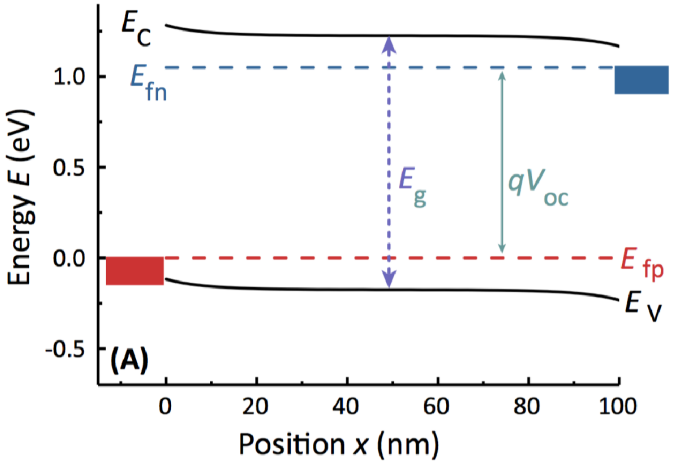

Figure 2: Band energy diagram of a solar cell when operating at open circuit. E_C and E_V are the energy levels of the conduction and valence bands respectively, and E_g is the bandgap energy. The red and blue rectangles are the anode and cathode Fermi levels and the difference between these is the V_{OC} [4].

Fill Factor (FF)

The J_{SC} and the V_{OC} are important figures of merit, but the device is not operational at either of these points since the net power would be zero. The Fill Factor (FF) is a parameter that helps characterise a solar cell. It represents the 'ideality' of a PV device and is defined as the ratio between the maximum power and the theoretical maximum power [8].

$$FF = \frac{V_{MAX}\, J_{MAX}}{V_{OC}\, J_{SC}} \quad \text{Eq. 6}$$

Graphically, it represents the squareness of the J-V curve of a solar cell and is the ratio between the rectangle with the biggest area that can be fit inside the J-V curve and the area of the rectangle defined by the V_{OC} and J_{SC} (see Figure 3).

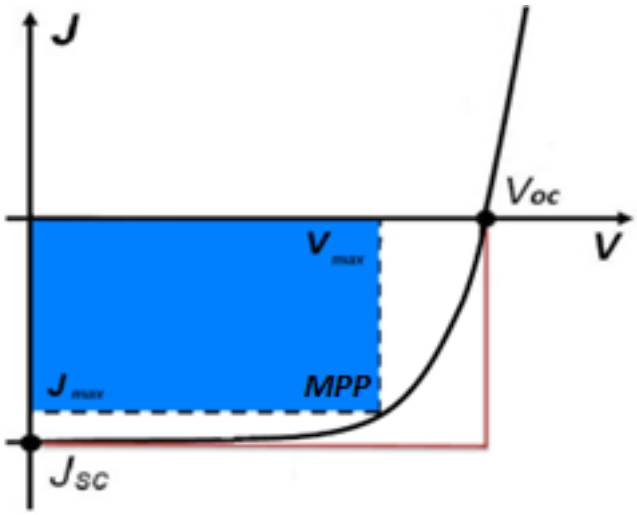

Figure 3: Graphic representation of the Fill Factor. The rectangle with the largest area (in blue) that can be adjusted to the J-V curve of a solar cell, which defines J_{MAX}, V_{MAX}, and P_{MAX}. The ratio between this rectangle and the one formed by the J_{SC} and V_{OC} values (red line) corresponds to the FF.

Power Conversion Efficiency (PCE)

The power conversion efficiency of a solar cell is the percentage of current generated with respect to the amount of incident light. It is defined as the ratio between the maximum power and the incident power, which can be rewritten in terms of V_{OC}, J_{SC}, and FF.

$$PCE = \frac{P_{MAX}}{P_{IN}} = \frac{V_{OC}\, J_{SC}\, FF}{P_{IN}} \qquad \text{Eq. 7}$$

Effects of Temperature

The bandgap normally decreases as temperature increases due to thermal expansion of the atomic lattice and changes in the phonon-electron interaction (see Figure 4). For smaller band gaps, it is easier to excite electrons from the VB since less energy is required. This translates into an increase in the photocurrent generated, but there will be more recombination, meaning the electrons fall back into their original state, increasing radiative losses. The increase in temperature will also affect the number of electrons locally present in the material. The population of electrons will increase exponentially, causing an increase in the dark current density, which negatively impacts the V_{OC}.

Despite the increase in photocurrent, the efficiency of the solar cell decreases because the loss in voltage outweighs the gains in current (see Figure 5).

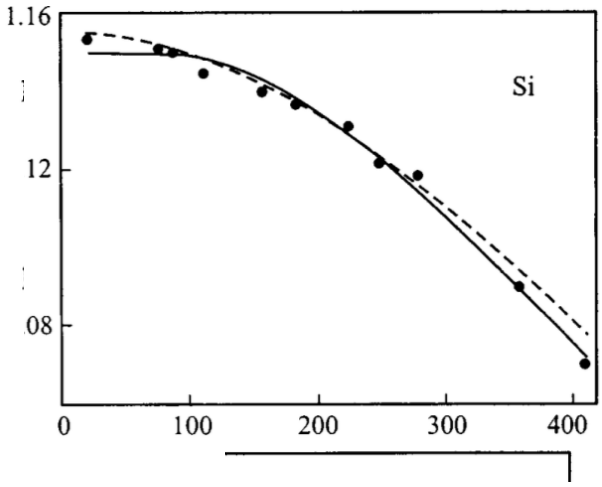

Figure 4: Temperature dependence of the band gap of Si [20].

Given the relationship between band gap and voltage (see Figure 2.1), the voltage will also be affected by temperature variations. The effects of temperature are mostly visible in the output voltage. V_{OUT} decreases as the temperature increases. This is a well-known effect that has been studied. Figure 1 shows how voltage decreases for different temperatures, represented in the IV curve. Consequently, the effects on voltage will also affect the output power, see Figure 6, and therefore, the efficiency of the solar cell decreases as well as its overall performance [4-13].

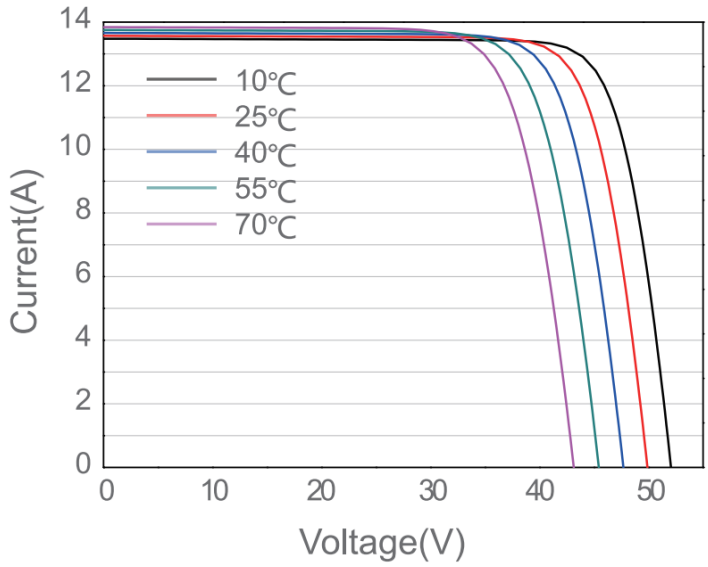

Figure 5: J-V curves of a commercial PV panel for different temperatures. As the temperature increases, the voltage available in the device decreases [14].

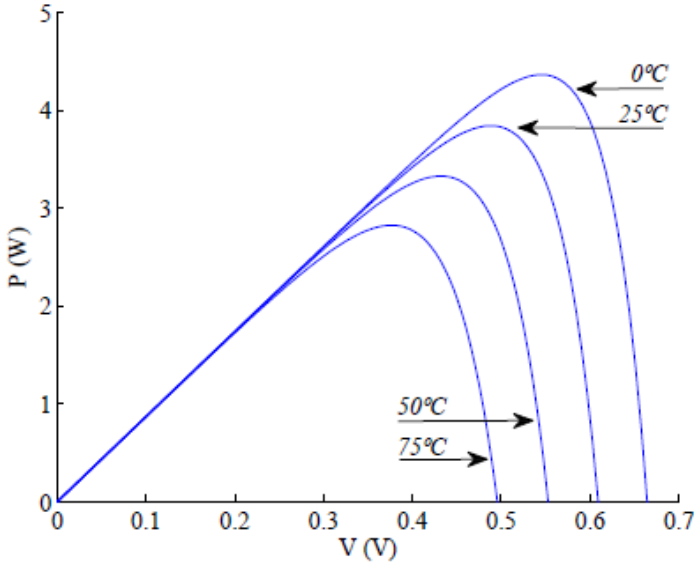

Figure 6: P-V curves of an ideal solar cell for different temperatures. As the temperature increases, the maximum power output from the device decreases [15].

Characteristics and Technical Description

Nowadays, the most common type of PV devices are made from crystalline silicon (c-Si), which completely dominates the solar cell market with more than 95% of the total shares of sold solar modules [17]. Therefore, E.ON's PV panel series JAM72S30 525-

550/MR/1500V is taken as a standard commercial reference product for a Si panel. The physical characteristics of these devices are shown in **Table 1** [14,16]. Based on the information provided by the manufacturer and the available data sheets, the expected performance of the devices is shown in **Figure 8**.

Table 1: Physical characteristics of commercial solar panels.

	Individual Layers		Units
Material	Silicon	Glass	
Length	2.28	2.28	m
Width	1.13	1.13	m
Thickness	0.19	3.5	mm
Specific Heat	710	810	J/kg K
Absorptivity	90	15	%
	Complete Device		
Rated Power	550		W
Voc	49.90		V
Max Power Voltage	41.90		V
Jsc	14		A
Max Power Current	13.11		A
Efficiency	21.3		%
	Conditions for cooling		
Inlet water temperature	25		°C
Outlet water temperature	60		°C
Solar irradiance	1000		W/m^2

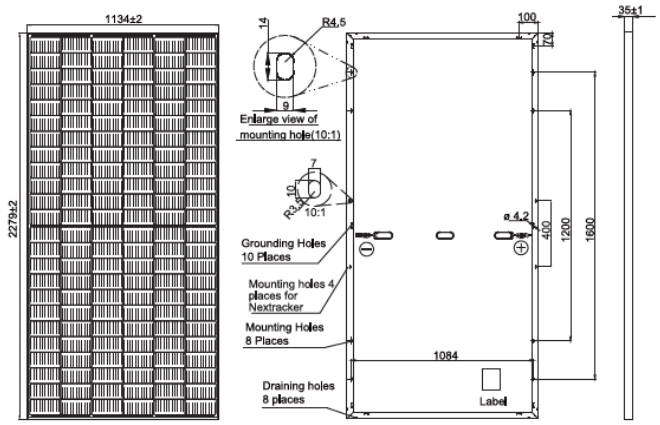

Figure 7: Mechanical Diagram of PV Panel from E.ON (JAM72S30) series [14].

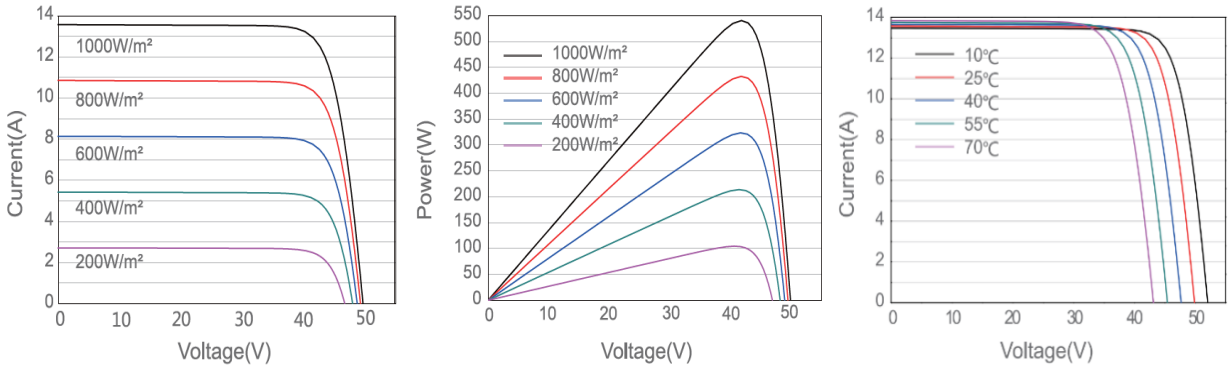

Figure 8: Expected performance of commercial reference product for a Si panel [14].

The water flow rate required to keep the panel's surface temperature at 25 °C is approximately 0.016 l/s = 57.5 l/h. This value was estimated following **Eq. 8.** and the conditions shown in Table 1 [18]**.**

$$\dot{Q} = G\,\alpha\,A = \dot{m}\,C_p\,\Delta T \qquad \text{Eq. 8}$$

where Q is the heat flow rate, G is the solar irradiance, α is absorptivity, A is the contact surface area, m is the mass flow rate, Cp is the specific heat of the material, and ΔT is the temperature difference between the inlet and outlet for the cooling water.

The total cooling time will be determined by the physical design and limitations of the pipes and materials used to build the panel. The efficient use of pieces, materials, optimisation of available space, and avoidance of intrinsic and complex designs will be prioritised over faster cooling times. The use of copper or carbon steel pipes is suggested due to their efficient heat transfer properties. The pipes will either run between the encapsulant ethylene vinyl acetate (EVA) layer and the back sheet of the panel or behind the back sheet to optimise direct cooling of the active layer. The latter will simplify manufacturing but might be less effective when cooling the device.

The additional electricity generated by cooling a commercial solar panel was calculated based on the meteorological conditions in Lund, Sweden [21]. The results of these calculations are presented in Table 2.

Table 2: Energy gains by cooling down a panel in Lund, Sweden.

Month	Panel Surface Temp (°C)	Nominal Power (W)	Monthly Energy Output (kWh)	Monthly Output @ 25°C (kWh)	Gain (kWh)	Gain (%)
Jan	27	549.23	6.77	6.82	0.05	0.70
Feb	27	549.04	9.18	9.24	0.06	0.70
Mar	31	544.23	30.05	30.69	0.64	2.15
Apr	36	536	52.35	54.45	2.10	4.00
May	41	527	83.70	88.66	4.96	5.93
Jun	44	520.55	97.04	103.95	6.91	7.12
Jul	46	515.35	97.94	105.71	7.77	7.93
Aug	45	516.89	82.45	88.66	6.21	7.53
Sep	41	523.05	59.19	62.7	3.51	5.93
Oct	37	532.10	32.67	34.1	1.43	4.38
Nov	32	539.80	12.87	13.2	0.32	2.51
Dec	29	545.95	6.72	6.82	0.10	1.42
Average	**36.33**	**533.25**	**47.57**	**50.41**	**2.84**	**5.97**
Total/year			**570.93**	**605.00**	**34.07**	**5.97**

Significant improvements occur during the hottest months of the year; between June and August, when the solar panel's performance increases by approximately 7% to 8% per month. On an annual basis, each panel experiences an overall gain of 6%. Consequently, for a potential installation of 3.5 MW that generates approximately 4 GWh of electricity per year, an additional 240 MWh can be obtained by cooling the panels. This is the equivalent of the yearly electricity consumption of 100 apartments in Lund, Sweden, approximately. (See Appendix 3 for more detailed calculations of these results).

Benchmarks

To gain a better perspective on the current state of this technology, product benchmarks were analysed and a review of comparable technologies on the market was conducted. This included reaching out to companies specialising in hybrid PV-thermal systems.

Two companies that develop solar-thermal panels were contacted as part of this investigation: NakedEnergy[1] and Dualsun[2]. Both companies focus primarily on thermal energy generation rather than electricity production. Their systems are not designed to optimise performance through active panel cooling; therefore, while some electricity is generated, the primary objective of their products is thermal energy production.

A comparative performance analysis was carried out between a conventional photovoltaic system and a hybrid system, considering the specific operational and environmental conditions of ESS. The results are shown in Table 3.

Both systems' production is comparable when considering the total output, but considering only electricity production, the hybrid system falls short compared to the conventional. The conventional system's nominal output power per m^2 is 1.7 times bigger than the hybrid's, yet it produces 3.7 times more electricity per m^2 than its hybrid counterpart. This suggests that electricity generation is hindered (or, at least, not benefited) when the objective of the device is generating heat rather than cooling or exclusively generating electricity. This could also be due to simply better PV modules in the conventional system but taking into account that the conditions are the same for both, the expected performance should not deviate that much from the initial difference in output power per area.

Table 3: Performance comparison between a conventional PV system vs hybrid system.

	PV-Thermal	E.ON	units
Panel Size	0.573	2.5	m^2
Output power/m^2	130	220	W/m^2
Total Installation Area	24 700	15 180	m^2
Installed Capacity	2 309	3 248	kW
Total Electric Prod	1.6	3.7	GWh/year
Total Thermal Prod	1.9	0	GWh
Total CAPEX	20	2	M €
Electricity prod/m^2	65	244	kWh/m^2
ROI	25	7	years

[1] https://nakedenergy.com/
[2] https://dualsun.com/se/

Studies using phase change materials (PCM) as well as front-face water cooling also served as benchmarks, providing reference points for possible outcomes [18,19].

Front face cooling seems to be the most effective way of regulating and reducing the temperature of the panel to 35 °C by activating the water spraying system when the device reached 60 °C. Using a PCM provided consistent results in lowering the panel's temperature down to 35 °C – 45 °C, but the behaviour of the system varied depending on the configuration of the installation. When the panel was installed with an inclination of 42 degrees, the upper area of the system overheated, with a temperature difference of 50 °C. If the panel was installed horizontally, then the panel cooled in a uniform way. A comparison of these different cooling methods is shown in **Table 4**.

Table 4: Comparison between different cooling methods for PV.

	Standard PV	PCM	Front-Face cooling	Units
Panel Size	2.57	0.6	1.28	m^2
Output power/m2	214	166	144	W/m^2
Electricity Production	1.71	0.36	0.58	kWh/day
Thermal Production	0	2.5	0	kWh/day
Length	2.28	1.2	1.6	m
Width	1.13	0.5	0.8	m
Thickness	35	> 65	50	mm
Weight	28.6	33	15.4	kg
Rated Power	550	100	185	W
Voc	49.90	21.6	44.8	V
Max Power Voltage	41.90	18.7	36.5	V
Jsc	14	5.8	5.5	A
Max Power Current	13.11	5.4	5.1	A
Efficiency	21.3	15.6	14.7	%
Target temperature	25	35 – 45	35	°C
Max temp reached	60	90	45	°C
Solar irradiance	1000	1000	1000	W/m^2
Gains due to cooling	No Cooling	1.4	3.4	% / year

Conclusions

The negative impact that high temperatures (> 60 °C) have on the performance of PV panels is a well-known issue. Mitigation techniques that maintain the temperature within the range of 25 °C – 40 °C will enhance the performance of the PV panels and increase the energy output of a solar installation.

Hybrid PV-thermal panels are already available on the market. As previously stated, these devices are not designed to optimise performance through active cooling but rather generate heat as efficiently as possible; therefore, while some electricity is generated, the primary output of their products is thermal energy. Comparing these dual devices vs conventional solar PV panels, the electricity output of the conventional panel is higher, and the installation complexity and costs are lower. Hybrid technologies produce up to three times more energy per area than conventional devices if both thermal and photovoltaic production are considered. However, for installations whose main objective is electricity production rather than thermal energy, the dual devices currently available on the market require a higher investment and do not provide additional benefits compared to conventional PV panels.

Regarding cooling techniques, front face cooling seems to be a very effective way of lowering the temperature of the panel's surface, but it implies spraying or dripping water on top of the front of the device. As a long-term solution, having water not flow through a controlled environment (like pipes) will increase losses and will reduce the consistency and stability of the results. Running cooling water through built-in pipes at the back of the panel seems to be the most effective method, given its high reliability, robustness, and long-term stability. It will also simplify monitoring and data collection of the cooling system.

Using a phase change material (PCM) as a cooling agent instead of water appears to be an effective solution as well. One of the main problems encountered when using a PCM is that the panel overheats from the top if it is installed at an angle. This behaviour is not present when the panel is installed horizontally, only when the panel has an inclination. By pumping water from the bottom upwards instead of a PCM, this issue should be mitigated. Further analysis will be made to confirm this behaviour.

A solar panel that operates within a stable temperature range (e.g., 25°C – 45 °C) will perform better than one exposed to higher temperatures, resulting in increased energy yield. A thermally stable solar panel will outperform a conventional device, thereby increasing its energy yield. While devices that combine photovoltaic and solar thermal technologies are available, they do not offer a significant advantage over conventional PV panels in terms of electricity generation. Therefore, they are not a viable option given their higher cost and lower electrical energy yield. A panel that prioritises cooling rather than heat generation has a higher potential than the hybrid PV-thermal devices since the electricity output will be improved significantly, especially during hot seasons. This type of device should perform better than the conventional PV panel and the hybrid PV-thermal, in terms of electricity production solely. As suggested by the calculations in Table 2, for a solar energy installation at a RI (typically characterized by installed capacities in the MW range and annual production in the order of GWh), a gain of hundreds of MWh every year can be achieved if the temperature is consistently maintained at around 25°C.

A prototype will be built to test this hypothesis and verify whether the benefits of cooling down the panel are significantly higher than those achieved under conventional operating conditions and those obtained with hybrid PV-thermal technology.

References

1. CORDIS-EU. (2025, May 25). Flexibility in RIs for global carbon neutrality fact sheet. European Commission. Retrieved February 10, 2025, from https://cordis.europa.eu/project/id/101131516
2. FlexRICAN. (2025, May). About FlexRICAN. Retrieved February 10, 2025, from https://flexrican.eu/about-flexrican/
3. FlexRICAN. (2025, May). Work package 3. Retrieved February 10, 2025, from https://flexrican.eu/about-flexrican/
4. Azzouzi, M., Kirchartz, T., & Nelson, J. (2019). Factors controlling open-circuit voltage losses in organic solar cells. Trends in Chemistry, 1(1), 49–62. https://doi.org/10.1016/j.trechm.2019.01.010
5. Grundmann, M. (2016). The physics of semiconductors (3rd ed.). Leipzig, Germany: Springer. https://doi.org/10.1007/978-3-319-23880-7
6. Van Vechten, J. A. (1990). A simple man's view of the passivation of semiconductors. Corrosion Sterne, 31, 39–52.
7. Van Vechten, J. A., & Malloy, K. J. (1990). The temperature dependence of band offsets for semiconductor heterojunctions in general and for the particular cases of AlAs–GaAs and HgTe–CdTe. Journal of Physics: Condensed Matter, 2, 281–293. https://doi.org/10.1088/0953-8984/2/2/004
8. Nelson, J. (2007) The physics of solar cells (5th ed.) London, Imperial College Press
9. Würfel, P., & Würfel, U. (2016). Physics of solar cells: From basic principles to advanced concepts (3rd ed.). Weinheim, Germany: Wiley-VCH.
10. Martínez, M. T., & Moctezuma, C. L. (2006). Métodos fisico-químicos en biotecnología: Espectrofluorimetría. Temas y Métodos. UAM, 67.
11. Blanche, P. (2016). Photorefractive organic materials and applications. Switzerland: Springer. https://doi.org/10.1007/978-3-319-29334-9
12. Brütting, W. (2005). Physics of organic semiconductors. Weinheim, Germany: Wiley-VCH Verlag GmbH & Co. KGaA.

13. Rudan, M. (2015). Physics of semiconductor devices. Switzerland: Springer. https://doi.org/10.1002/3527606637
14. JA Solar. (2021). JAM72S30 525-550/MR/1500V series data sheet (Version Global_EN_20210607A).
15. Rodrigues, E. M. G., Melício, R., Mendes, V. M. F., & Catalão, J. P. S. (2011). Simulation of a solar cell considering single-diode equivalent circuit model. Renewable Energies and Power Quality Journal, 9(1). https://doi.org/10.24084/repqj09.339
16. Santbergen, R. (2008). The absorption factor of crystalline silicon PV cells: A numerical and experimental study. Solar Energy Materials and Solar Cells, 92(4), 432–444. https://doi.org/10.1016/j.solmat.2007.10.005
17. Fraunhofer ISE , (2021, July 27). Photovoltaics report. Retrieved March 08, 2025, https://www.ise.fraunhofer.de/content/dam/ise/de/documents/publications/studies/Photovoltaics-Report.pdf
18. González-Peña, D., Melício, R., Mendes, V. M. F., & Catalão, J. P. S. (2020). Experimental analysis of a novel PV/T panel with PCM and heat pipes. Sustainability, 12, 1710. https://doi.org/10.3390/su12051710
19. Moharram, K. A. (2013). Enhancing the performance of photovoltaic panels by water cooling. Engineering Journal, 4, 869–877. http://dx.doi.org/10.1016/j.asej.2013.03.00
20. Vainshtein, IA & Zatsepin, Anatoly & Kortov, Vsevolod. (1999). Applicability of the empirical Varshni relation for the temperature dependence of the width of the band gap. Physics of The Solid State. 41. 905-908. http://dx.doi.org/10.1134/1.1130901.
21. Sveriges meteorologiska och hydrologiska institute (SMHI). Temperatur och vind. Retrieved March, 2025, from https://www.smhi.se/data/temperatur-och-vind

Appendices

Appendix 1: Geographical Conditions in Lund, Sweden

- Longitude: 13.247
- Latitude: 55.734
- Elevation: 80 m
- 1000 sun peak hours (annual average)

Appendix 2: Meteorological data

Meteorological data from a typical meteorological year (TMY) is shown in Figure 9.

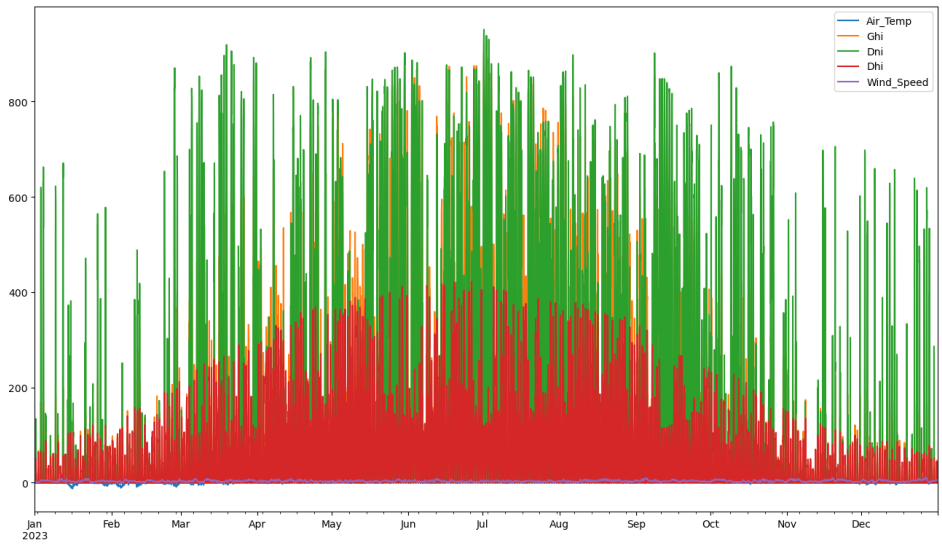

Figure 9. *Meteorological data from a typical meteorological year (TMY) for Lund. Data taken from Photovoltaic Geographical Information System (PVGIS).*

Note: Approximate annual electricity consumption of an apartment: 2,500 kWh. *Source: The Little Energy Saving Book – E.ON*

Appendix 3: Energy gains by cooling down a panel calculations.

A more detailed version of the calculations shown in Table 2 is presented in Figure 10a. The air temperature high averages were taken for the calculations shown in Table 2. A more conservative estimation of these results is shown in Figure 10b.

a)

Month	Days	Ambient Temp (°C)	Panel Temp (°C)	ΔT (°C)	Power (W)	Adjusted Power (W/m²)	Irradiance (kWh/m²/day)	Average monthly ghi (kWh/m²/month)	Nominal Energy hitting the panel (kWh)	Ideal Energy Output (kWh)	Adjusted Energy (kWh)	Gain (kWh)	Gain (%)
Jan	31	2	27	2	546.15	218.46	0.4	12.4	31	6.82	6.77226	0.05	0.70
Feb	28	2	27	2	546.15	218.46	0.6	16.8	42	9.24	9.17532	0.06	0.70
Mar	31	6	31	6	538.45	215.38	1.8	55.8	139.5	30.69	30.04551	0.64	2.15
Apr	30	11	36	11	528.825	211.53	3.3	99	247.5	54.45	52.353675	2.10	4.00
May	31	16	41	16	519.2	207.68	5.2	161.2	403	88.66	83.69504	4.96	5.93
Jun	30	19	44	19	513.425	205.37	6.3	189	472.5	103.95	97.037325	6.91	7.12
Jul	31	21	46	21	509.575	203.83	6.2	192.2	480.5	105.71	97.940315	7.77	7.93
Aug	31	20	45	20	511.5	204.6	5.2	161.2	403	88.66	82.4538	6.21	7.53
Sep	30	16	41	16	519.2	207.68	3.8	114	285	62.7	59.1888	3.51	5.93
Oct	31	12	37	12	526.9	210.76	2	62	155	34.1	32.6678	1.43	4.38
Nov	30	7	32	7	536.525	214.61	0.8	24	60	13.2	12.8766	0.32	2.51
Dec	31	4	29	4	542.3	216.92	0.4	12.4	31	6.82	6.72452	0.10	1.42
Total/year		4	29	4	542.3	216.92	0.4	12.4	2750.00	605.00	570.930965	34.069035	5.97
		36.3333333	11.33333	528.1833333									

b)

Month	Days	Ambient Temp (°C)	Panel Temp (°C)	ΔT (°C)	Power (W)	Adjusted Power (W/m²)	Irradiance (kWh/m²/day)	Average monthly ghi (kWh/m²/month)	Nominal Energy hitting the panel (kWh)	Ideal Energy Output (kWh)	Energy with Thermal Losses (kWh)	Gain (%)
Jan	31	0.4	25.4	0.4	549.23	219.692	0.4	12.4	31	6.82	6.810452	0.14
Feb	28	0.5	25.5	0.5	549.0375	219.615	0.6	16.8	42	9.24	9.22383	0.18
Mar	31	3	28	3	544.225	217.69	1.8	55.8	139.5	30.69	30.367755	1.06
Apr	30	7.3	32.3	7.3	535.9475	214.379	3.3	99	247.5	54.45	53.0588025	2.62
May	31	12	37	12	526.9	210.76	5.2	161.2	403	88.66	84.93628	4.38
Jun	30	15.3	40.3	15.3	520.5475	208.219	6.3	189	472.5	103.95	98.3834775	5.66
Jul	31	18	43	18	515.35	206.14	6.2	192.2	480.5	105.71	99.05027	6.72
Aug	31	17.2	42.2	17.2	516.89	206.756	5.2	161.2	403	88.66	83.322668	6.41
Sep	30	14	39	14	523.05	209.22	3.8	114	285	62.7	59.6277	5.15
Oct	31	9.3	34.3	9.3	532.0975	212.839	2	62	155	34.1	32.990045	3.36
Nov	30	5.3	30.3	5.3	539.7975	215.919	0.8	24	60	13.2	12.95514	1.89
Dec	31	2.1	27.1	2.1	545.9575	218.383	0.4	12.4	31	6.82	6.769873	0.74
Total/year			33.7	8.7	533.2525				2750.00	605.00	577.496293	4.76

Figure 10a and 10b. Full calculations and more conservative estimations of the calculations shown in Table 2, side by side